© 2014. Published by The Company of Biologists Ltd | Journal of Cell Science (2014) 127, 5093–5104 doi:10.1242/jcs.159772

RESEARCH ARTICLE

Coupled synthesis and translocation restrains polyphosphate to acidocalcisome-like vacuoles and prevents its toxicity

Rūta Gerasimaitė[‡], Shruti Sharma[*,‡], Yann Desfougères, Andrea Schmidt and Andreas Mayer[§]

ABSTRACT

Eukaryotes contain inorganic polyphosphate (polyP) and acidocalcisomes, which sequester polyP and store amino acids and divalent cations. Why polyP is sequestered in dedicated organelles is not known. We show that polyP produced in the cytosol of yeast becomes toxic. Reconstitution of polyP translocation with purified vacuoles, the acidocalcisomes of yeast, shows that cytosolic polyP cannot be imported, whereas polyP produced by the vacuolar transporter chaperone (VTC) complex, an endogenous vacuolar polyP polymerase, is efficiently imported and does not interfere with growth. PolyP synthesis and import require an electrochemical gradient, probably as a driving force for polyP translocation. VTC exposes its catalytic domain to the cytosol and carries nine vacuolar transmembrane domains. Mutations in the VTC transmembrane regions, which are likely to constitute the translocation channel, block not only polyP translocation but also synthesis. Given that they are far from the cytosolic catalytic domain of VTC, this suggests that the VTC complex obligatorily couples synthesis of polyP to its import in order to avoid toxic intermediates in the cytosol. Sequestration of otherwise toxic polyP might be one reason for the existence of acidocalcisomes in eukaryotes.

KEY WORDS: Yeast vacuole, Inorganic polyphosphate, VTC complex, Acidocalcisome

INTRODUCTION

Inorganic polyphosphate (polyP) is a polymer of orthophosphate units linked together by high-energy phospho-anhydride bonds. It is present in all organisms tested so far (Rao et al., 2009). The hallmark of polyP metabolism in eukaryotic organisms is the concentration and enclosure of polyP in membrane-bound compartments, acidocalcisomes. Acidocalcisomes share a number of highly conserved features. They are acidic compartments that accumulate polyphosphate, basic amino acids, polyamines, Ca^{2+}, Zn^{2+}, Mg^{2+} and Mn^{2+} ions to high concentrations (Docampo and Moreno, 2011). In trypanosomatids, acidocalcisomes are important for osmoregulation and Ca^{2+} signaling (Docampo et al., 2010; Huang et al., 2013). Adaptor protein complex-3 and TOR3 kinase have been implicated in acidocalcisome biogenesis (Besteiro et al., 2008; de Jesus et al., 2010; Madeira da Silva and Beverley, 2010; Huang et al., 2011). However, many aspects of the biogenesis and metabolic roles of acidocalcisomes are still poorly understood.

In prokaryotes, the roles and the enzymes involved in polyP synthesis and degradation are well characterized. The bacterial polyphosphate kinase (*Ec*Ppk1) mediates a reversible reaction in which it generates polyP by transferring the γ-phosphate of ATP (Ahn and Kornberg, 1990; Akiyama et al., 1992). The major polyP-degrading enzyme is an exopolyphosphatase (*Ec*Ppx1) (Bolesch and Keasling, 2000). Many important processes are influenced by polyP in bacteria, such as virulence, pathogenicity, stress response (Kim et al., 2002) and biofilm formation (Chen et al., 2002). PolyP was also shown to form membrane channels with poly-β hydroxybutyrate and Ca^{2+} (Reusch, 1989). Furthermore, polyP interacts with *Escherichia coli* Lon protease and promotes ribosomal protein degradation (Kuroda et al., 2001). Recently, polyP was recognized to act as a molecular chaperone in bacteria, which might explain the pleiotropic phenotypes and stress sensitivity that results from polyP deficiency (Gray et al., 2014).

In mammals, polyP is implicated in blood coagulation (Smith et al., 2006; Choi et al., 2011), apoptosis of activated plasma cells (Hernandez-Ruiz et al., 2006), bone mineralization (Hoac et al., 2013) and apatite formation (Omelon and Grynpas, 2011). PolyP is enriched in certain cancer cells (Jimenez-Nunez et al., 2012) and has been linked to the energy metabolism of mitochondria (Pavlov et al., 2010). PolyP might also modulate neuron excitability (Holmström et al., 2013; Stotz et al., 2014).

Most knowledge on polyP metabolism in eukaryotes comes from *Saccharomyces cerevisiae*, where three enzymes degrading polyP have been identified – the cytosolic exopolyphosphatase Ppx1, the cytosolic endopolyphosphatase Ddp1 and the vacuolar endopolyphosphatase Ppn1 (Wurst and Kornberg, 1994; Wurst et al., 1995; Sethuraman et al., 2001; Shi and Kornberg, 2005; Lonetti et al., 2011). The polyP-synthesizing enzyme Vtc4 is a part of the multi-subunit vacuolar transporter chaperone (VTC) complex (Hothorn et al., 2009). Vtc4 has homologs in lower eukaryotes but sequence comparisons have so far failed to identify homologs in plants or animals. Yeast Vtc4 is one of the three unrelated eukaryotic polyP-synthesizing enzymes known to date. The other two were found in *Dictyostelium discoideum* – PPK1 of bacterial origin (Zhang et al., 2007) and PPK2, similar to actin-related proteins (Gómez-García and Kornberg, 2004). VTC homologs are readily identifiable in parasitic protozoa (Rooney et al., 2011), where they are essentially localized in acidocalcisomes (Docampo et al., 2005). The ablation of VTC impairs growth (Fang et al., 2007), virulence and infectivity of *Trypanosoma brucei* (Lander et al., 2013), suggesting that VTC could be explored as a drug target. The VTC complex of yeast affects vacuole fusion (Müller et al., 2002), microautophagy (Uttenweiler et al., 2007) and trafficking of other proteins towards or through the Golgi (Müller et al., 2003), suggesting that

Department of Biochemistry, University of Lausanne, Ch. des Boveresses 155, 1066 Epalinges, Switzerland.
*Present address: Department of Biophysics, Bose Institute, P 1/12, C. I. T. Road, Scheme, VIIM Kolkata, 700054, West Bengal, India.
‡These authors contributed equally to this work

§Author for correspondence (andreas.mayer@unil.ch)

Received 15 July 2014; Accepted 8 October 2014

Journal of Cell Science

Journal of Cell Science (2014) 127, 5093–5104 doi:10.1242/jcs.159772

polyP synthesis in yeast might be integrated with other cellular functions.

The yeast VTC complex is membrane anchored (Müller et al., 2002). Vtc4 contains three transmembrane helices at its C-terminus. It localizes to the vacuole and the endoplasmic reticulum membranes (Hothorn et al., 2009). The large soluble part of Vtc4 faces the cytoplasm (Müller et al., 2003). It consists of a catalytic tunnel domain and an N-terminal SPX domain of unknown function. Owing to its topology, Vtc4 has access to the cytosolic nucleotide triphosphate pools and synthesizes polyP by transferring the γ-phosphate of nucleotide triphosphates onto growing polyP chains. The VTC complex contains two other subunits – Vtc2 (or, alternatively, its homolog Vtc3) and Vtc1. The VTC complex exists in two isoforms, Vtc1/3/4, which mainly localizes to vacuoles, and Vtc1/2/4, which is also very abundant in the endoplasmic reticulum (Hothorn et al., 2009). Vtc2 and Vtc3 are highly homologous to Vtc4 but their tunnel domains lack functional active sites. Vtc1 contains no cytoplasmic domain and consists of three transmembrane regions that are homologous to those of Vtc2, Vtc3 and Vtc4. A VTC complex thus contains at least nine transmembrane domains.

Most polyP in yeast is stored in vacuoles (Indge, 1968; Urech et al., 1978). Only a minor fraction (<10%) is associated with other organelles, such as mitochondria or the nucleus (Urech et al., 1978; Saito et al., 2005). Vacuoles show all the crucial characteristics of acidocalcisomes. They can be easily purified and therefore represent a model of choice for studies of acidocalcisome biogenesis and function and for investigating polyP metabolism.

Here, we posed the question of why polyP is generally sequestered within acidocalcisomes. We studied the effects of polyP mislocalization into the cytoplasm and established *in vitro* conditions permitting polyP synthesis by isolated yeast vacuoles. We used this system to explore how polyP is synthesized and transferred into the vacuole lumen.

RESULTS

Cytosolic polyP is toxic to yeast cells

Why is polyP sequestered in intracellular organelles? To determine whether cytosolic polyP could be deleterious to the cells, we sought to establish a cytosolic pool of polyP by expressing the heterologous polyphosphate kinase gene Ppk1 from *E. coli* (*Ec*Ppk1). This protein lacks signal sequences and thus was localized in the cytosol of yeast cells. Expression of *Ec*Ppk1 increased the polyP content of wild-type cells by ∼20% (Fig. 1A). In *vtc1Δ* cells, which lack a functional VTC complex and have barely detectable levels of polyP, *Ec*Ppk1 expression established a pool of polyP yielding a clearly detectable signal. The magnitude of this signal corresponded to the absolute increase in signal that the same *Ec*Ppk1 construct produced in a wild-type cell. Because yeast cells are known to contain ∼200 mM polyP (Auesukaree et al., 2004), we can estimate that polyP synthesized by *Ec*Ppk1 might reach up to ∼40 mM. *Ec*Ppk1-expressing cells showed a growth defect as compared with the wild-type cells (Fig. 1B), as well as an aberrant morphology (Fig. 1C). 10–15% of the population showed abnormal protrusions or were cone-shaped. However, these cells were still alive, as demonstrated by FUN-1® staining (Fig. 1D). Their survival might be due to the presence of the extremely potent cytosolic polyphosphatase Ppx1 (Wurst and Kornberg, 1994). In order to test this hypothesis, we took wild-type cells, replaced the endogenous promoter for *PPX1* with the glucose-repressible GAL1 promoter and introduced the plasmid expressing *Ec*Ppk1. These cells grew on galactose, which provided high expression of *PPX1*, but not on glucose, which repressed PPX1 (Fig. 1E,F). This suggests that polyP production in the cytosol is toxic to the cells in a Ppx1-dependent fashion.

PolyP synthesized by VTC does not accumulate in the cytosol

Given that the catalytic domain of the VTC complex is exposed to the cytoplasm (Müller et al., 2003), the polyP synthesized by it should be similarly deleterious for the cells as the polyP produced by expression of *Ec*Ppk1 in the cytosol. The cells might circumvent this problem by directly translocating nascent polyP into the vacuolar lumen and avoiding diffusible intermediates in the cytosol.

This hypothesis can be tested *in vivo* by artificially overexpressing a polyphosphatase in yeast cells. If the polyP synthesized by VTC does not accumulate in the cytosol but is immediately transferred into vacuoles, overexpression of a cytosolic polyphosphatase should have little effect. Conversely, artificial targeting of a polyphosphatase into the vacuoles might reduce cellular polyP content significantly. In order to target the polyphosphatase Ppx1 into the vacuole lumen, the 5′ end of the *PPX1* gene was fused to an N-terminal pre-pro-sequence of the vacuolar carboxypeptidase Y and expressed from the strong glyceraldehyde-3-phosphate dehydrogenase (GPD) promoter. The localization of the targeted protein in the vacuole was confirmed using a GFP tag (Fig. 2A). The levels of the polyP polymerase subunit Vtc4 were not affected by vacuole-targeted Ppx1 (Fig. 2B). Overexpressing vacuole-targeted Ppx1 reduced polyP content by 90% as compared with that of the wild-type strain (Fig. 2C). By contrast, if a cytosolic version of Ppx1 was overexpressed, polyP levels did not change at all. These results are consistent with the idea that polyP is rapidly translocated across the vacuolar membrane *in vivo* and that a significant intermediate pool in the cytosol might not exist.

Isolated yeast vacuoles synthesize polyP *in vitro*

We reasoned that purified vacuoles could serve as a model system to study polyP metabolism *in vitro*. We measured polyP production by the characteristic fluorescence emission of DAPI–polyP complexes at 550 nm (Kapuscinski, 1990; Aschar-Sobbi et al., 2008). Because the DAPI–polyP interaction is sensitive to sample composition (Diaz and Ingall, 2010; Martin and Van Mooy, 2013), we assessed the effects of lipids and other vacuole contents. Calibration curves of synthetic polyP with an average chain length of 60 (polyP-60) were measured in the presence or in the absence of vacuoles in which the enzymes had been inactivated by heating. Vacuolar compounds did not significantly influence the DAPI–polyP signal (Fig. 3A).

We tested whether isolated vacuoles can synthesize polyP by incubating them with an ATP-regenerating system (ATP-RS) at 27℃. $MnCl_2$ was included in the reaction because the Vtc4 catalytic domain binds Mn^{2+} in its active center. At different time points, the reaction was stopped by adding EDTA to sequester divalent cations, Triton X-100 to dissolve vacuole membranes and DAPI to detect polyP. DAPI–polyP fluorescence was assayed in a 96-well spectrofluorometer (Fig. 3B). The *in vitro* reaction showed an initial lag phase of ∼5 min, followed by a nearly linear increase in signal for the next 30 min. Vacuoles from a *vtc1Δ* strain did not increase their DAPI signal. The signal generated in wild-type samples depended on the presence of vacuoles. Its emission spectrum was identical to the spectrum of

Journal of Cell Science

Journal of Cell Science (2014) 127, 5093–5104 doi:10.1242/jcs.159772

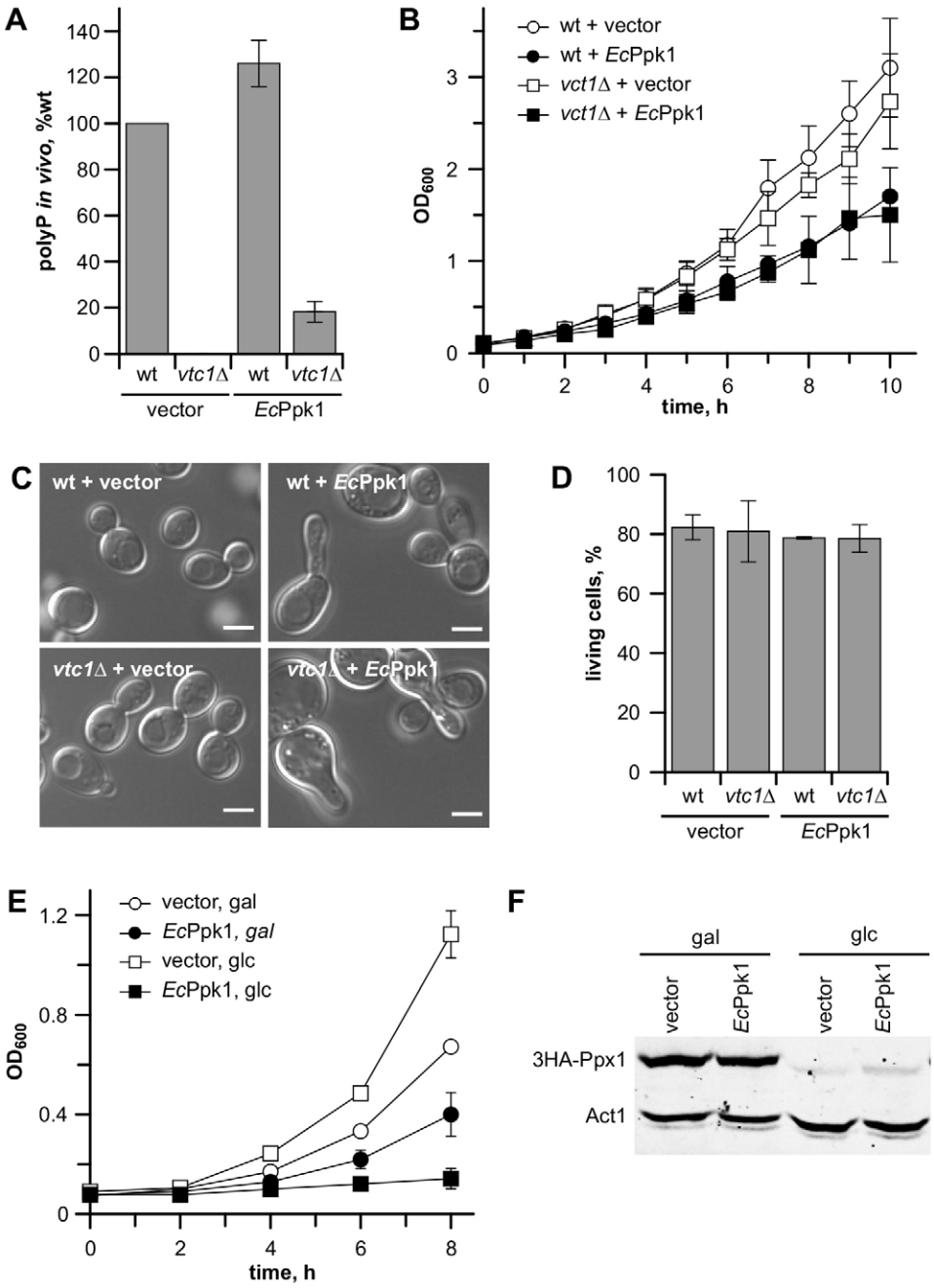

Fig. 1. Effects of cytosolic expression of a bacterial polyphosphate kinase (*Ec*Ppk1). (A–D) BJ3505 (wild-type; wt) or *vtc1*Δ cells carrying an empty vector or overexpressing a plasmid-encoded *Ec*Ppk1 were grown in HC^{-URA} medium and analyzed. (A) Accumulation of polyP *in vivo*. (B) Growth in liquid medium. Pre-cultures in 5 ml of medium (30˚C, 48 h) were diluted to an OD_{600} of 0.1, and OD_{600} was monitored over time. Experiments were performed at least in duplicates with at least two different transformants. (C) Cell morphology as determined by differential interference contrast (DIC) microscopy. Scale bars: 5 µm. (D) Quantification of viable cells by FUN-1 staining. (E) Growth arrest in the absence of Ppx1. BY4741 P_{GAL} 3×HA-Ppx1 cells were complemented with plasmid-encoded *Ec*Ppk1 or an empty vector and grown overnight in $HC^{-URA+GAL}$. Cells were harvested at an OD_{600} of 1, washed twice in $HC^{-URA+GAL}$ or $HC^{-URA+GLC}$, resuspended in the same medium at an OD_{600} of 0.05, incubated (30˚C, 24 h), diluted to an OD_{600} of 0.1 in the same medium and OD_{600} was monitored over time. Quantitative data show the mean±s.d. (F) Levels of 3HA–Ppx1 in extracts of cells used in E. Gal, galactose; glc, glucose.

the synthetic DAPI–polyP-60 complexes recorded under the same buffer conditions (Fig. 3C). PolyP did not accumulate if EDTA was included from the beginning or if only ATP but no ATP-regenerating system was present (Fig. 3B). The latter is likely because of the competition with V-ATPase for substrate ATP. Alternatively, this might point to a high sensitivity of the VTC complex to inhibition with the reaction product ADP, which is formed by VTC itself, V-ATPase or other ATPases on the vacuolar membrane.

PolyP synthesis was further confirmed by PAGE and negative staining of the gel with DAPI. A characteristic polyP ladder was observed for wild-type vacuoles incubated with an ATP-regenerating system (Fig. 3D). No polyP was detected in the gel if wild-type vacuoles had been incubated without ATP-regenerating system, in the presence of EDTA or if *vtc1*Δ vacuoles were used. Thus, isolated vacuoles synthesize polyP *in vitro*.

Synthesized polyP is translocated into the vacuolar lumen

Next, we determined whether the polyP synthesized by isolated vacuoles is translocated into their lumens. We based the translocation assay on the fact that the vacuolar membrane represents a barrier to DAPI. DAPI added to intact vacuoles should hence not stain polyP in their lumen. In order to test this, we allowed vacuoles to synthesize polyP, stopped the reaction with an EDTA-DAPI mixture and split the samples. One aliquot was left intact, the other one was immediately supplemented with Triton X-100, so as to dissolve the membranes and render all polyP accessible to DAPI. Aliquots with detergent showed 80% higher fluorescence than those with intact vacuoles (Fig. 4A).

Journal of Cell Science

Journal of Cell Science (2014) 127, 5093–5104 doi:10.1242/jcs.159772

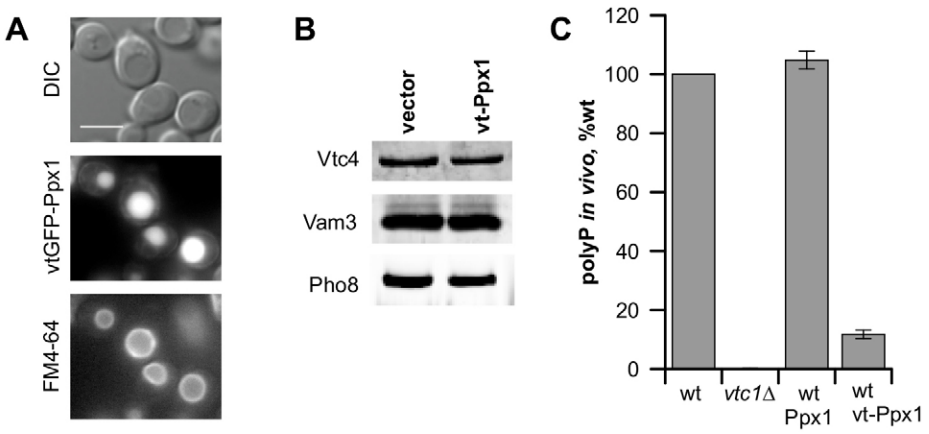

Fig. 2. The effects of Ppx1 overexpression on polyP accumulation *in vivo*. BJ3505 wt or *vtc1*Δ cells, carrying an empty vector or plasmids expressing the indicated proteins, were analyzed. (A) Vacuole-targeted (vt)-Ppx1 localizes to the vacuole. Wild-type (wt) cells expressing a GFP fusion of vacuole-targeted Ppx1 (vtGFP–Ppx1) were stained with FM-64 and analyzed by fluorescence and differential interference contrast (DIC) microscopy. Scale bar: 5 µm. (B) Expression of vt-Ppx1 does not change the abundance of Vtc4 on the vacuole membrane. Vacuoles were isolated from wild-type cells carrying an empty vector or a plasmid overexpressing vt-Ppx1. Proteins were analyzed by SDS-PAGE and western blotting; vacuolar proteins Vam3 and Pho8 were used as loading controls. (C) PolyP accumulation *in vivo*. The polyP content of wild-type cells was set to 100%. Data show the mean±s.d.

This increase in signal was not a side-effect of detergent addition because the detection of synthetic polyP-60 was not influenced by Triton X-100 (Fig. 4A). Furthermore, the detergent-dependent signal was not observed if the preceding incubation had been performed in the presence of EDTA or with *vtc1*Δ vacuoles, suggesting that it is not due to compounds other than the synthesized polyP. Thus, most of the synthesized polyP is inaccessible to DAPI because of the vacuolar membrane, suggesting that it is located in the vacuole lumen.

As a second criterion for translocation we tested whether the synthesized polyP is protected from degradation by externally added recombinant polyphosphatase Ppx1. Purified vacuoles were allowed to synthesize polyP *in vitro*, chilled and diluted in order to slow down polyP synthesis. Then, they were incubated in the presence or in the absence of purified Ppx1 on ice. Degradation was stopped by adding EDTA, Triton X-100 and DAPI, and DAPI–polyP fluorescence was measured (Fig. 4B). The large majority of polyP survived this treatment. Disrupting the integrity of the vacuoles by boiling rendered this polyP accessible for degradation. Furthermore, when similar amounts of synthetic polyP-60 were added to mutant vacuoles that are unable to synthesize polyP (*vtc1*Δ), the added polyP-60 was completely degraded by Ppx1. This confirms that the recombinant Ppx1 is sufficiently active to completely degrade the observed quantities of polyP if they are accessible.

As a third approach, we isolated vacuoles from the strain overexpressing Ppx1 with a vacuolar-targeting sequence. If polyP became translocated into the lumen of vacuoles, the presence of lumenal Ppx1 should reduce the apparent rate of polyP accumulation *in vitro*. Indeed, the apparent polyP synthesis *in vitro* was reduced by 90% (Fig. 4C), although these vacuoles had similar levels of Vtc4 to the wild-type controls (Fig. 2B). Taken together, these results suggest that polyP is not only synthesized by purified vacuoles but is also efficiently translocated into the vacuolar lumen.

PolyP synthesis by purified vacuoles requires an electrochemical potential

The translocation of polymers across a membrane requires a driving force. In addition, polyP is negatively charged. Its transport should be electrogenic and might require charge compensation by uptake or release of cations or anions, respectively. We tested the possibility that the electrochemical potential across the vacuolar membrane, which is maintained by the V-type H^+-ATPase, could provide a driving force for polyP translocation. We tested the effects of the V-ATPase inhibitor concanamycin A and of the protonophore FCCP, both of which interfere with the proton gradient across the vacuolar membrane. Both agents strongly inhibited polyP synthesis by intact vacuoles (Fig. 5A). As a complementary approach, we assayed polyP synthesis by vacuoles lacking subunit a of the V-ATPase, Vph1, in which vacuolar acidification is strongly reduced (Perzov et al., 2002). *vph1*Δ vacuoles contained the same amount of Vtc4 as wild-type vacuoles (Fig. 5B), but their polyP synthesis capacity was reduced to <20% of the wild-type value (Fig. 5C). These results underscore the importance of the proton gradient for polyP synthesis and are in line with information from high-throughput screens for polyP-deficient mutants, which have identified >250 candidate genes and among them several V-ATPase subunits (Freimoser et al., 2006).

Full catalytic activity of the VTC complex requires an intact membrane environment

Because the vacuolar proton gradient energizes many vacuolar ion transporters, it could facilitate the import of necessary counter-ions and prevent the buildup of an inverse electrical potential that would impede further polyP import. In this case, disruption of vacuolar integrity might render polyP synthesis independent of V-ATPase activity or even stimulate it. We therefore measured the effects of solubilization of the vacuolar membrane on the activity of the VTC complex. From a range of detergents tested, CHAPS allowed efficient solubilization of the VTC complex. Around 60% of VTC proteins were recovered in the solubilisate. When immunoprecipitated from the solubilisate, the subunits of the VTC complex were present in similar ratios to those observed in the intact vacuoles (Fig. 6A), suggesting that the complex remained intact. The amount of Vtc4 in the reaction was determined by western blotting using a pure recombinant Vtc4 catalytic domain ($Vtc4^{189–480}$) as a standard and an affinity-purified anti-Vtc4 rabbit polyclonal antibody. According to this comparison, vacuoles contain 1 pmol of Vtc4 per 1 µg of protein.

Journal of Cell Science

Journal of Cell Science (2014) 127, 5093–5104 doi:10.1242/jcs.159772

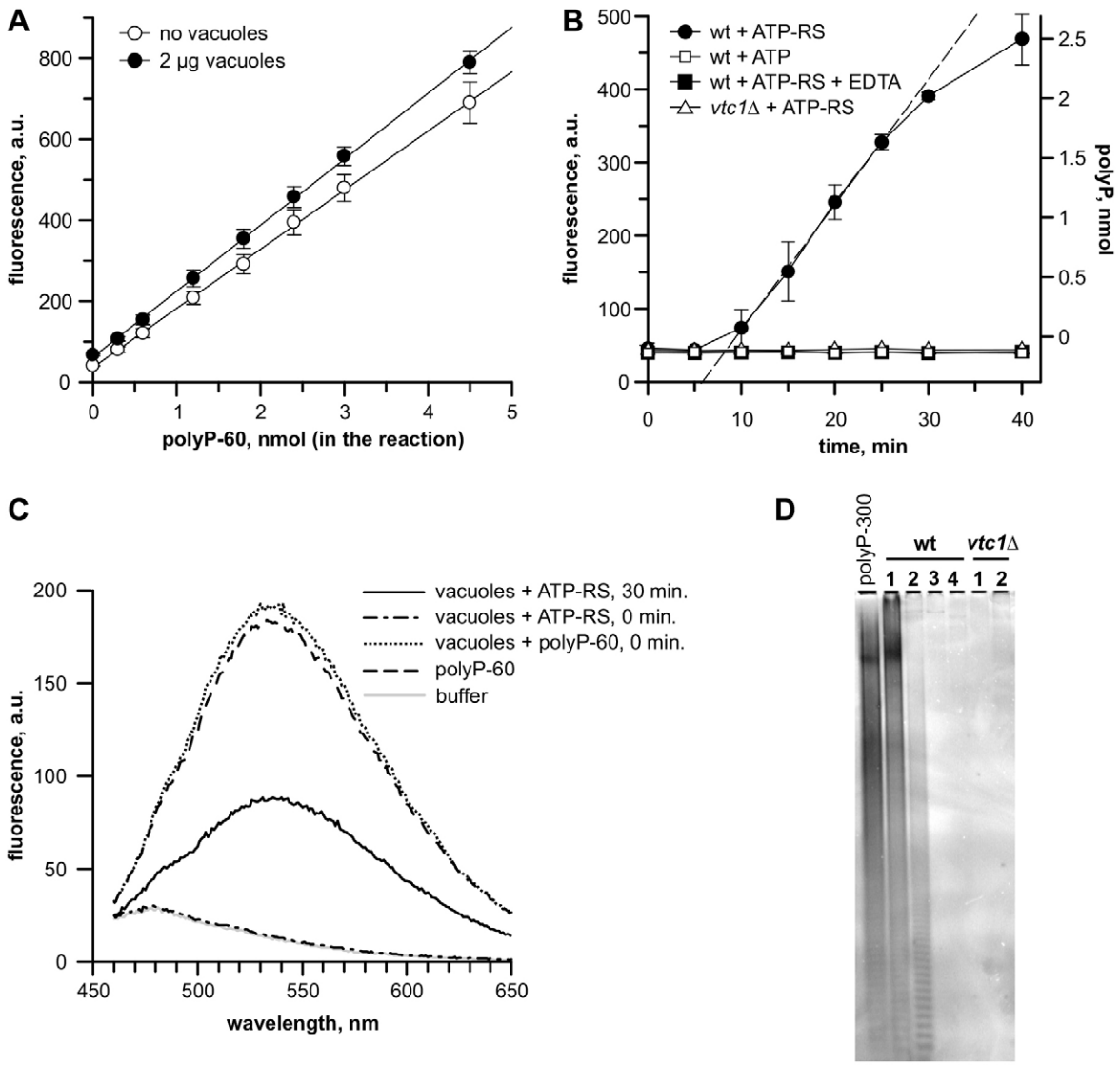

Fig. 3. Isolated yeast vacuoles synthesize polyP *in vitro*. (A) Fluorescence of increasing concentrations of polyP-60 was measured in the reaction mixture without or with 2 µg of heat-inactivated BJ3505 vacuoles. a.u., arbitrary units. (B) Purified vacuoles were incubated with ATP-RS, the reactions were stopped at the indicated time-points and DAPI–polyP fluorescence was measured as described in Materials and Methods. The linear phase of polyP synthesis allows estimating the apparent turnover rate of the vacuoles (dashed line, 0.05 nmol·µg^{-1}·min^{-1}). wt, vacuoles isolated from wild-type cells. Data show the mean±s.d. (C) Fluorescence emission spectra of DAPI–polyP under reaction conditions. The samples were prepared in the synthesis reaction mixture, incubated for 30 min at 27°C and stopped. In the '0 min' samples, vacuoles were added after the stop solution. (D) PAGE of polyP synthesized *in vitro* and *in vivo*. PolyP was extracted from whole cells (lanes 1), from vacuoles incubated with ATP-RS (lanes 2), from vacuoles without incubation (lane 3) or from vacuoles incubated with ATP-RS and 8 mM EDTA (lane 4). PolyP was purified from whole cells by glass beads and phenol extraction, and was ethanol-precipitated as described previously (Lonetti et al., 2011); before fractionation, the samples were sequentially treated with RNase A and proteinase K. PolyP was synthesized in a 600-µl reaction mixture containing 24 µg vacuoles for 1 h at 27°C. The samples were extracted with phenol:chloroform:isoamyl alcohol followed by chloroform and precipitated with ethanol. 7–20 pmol of polyP was fractionated in a 20% polyacrylamide gel, and polyP was visualized by negative DAPI staining (Smith and Morrissey, 2007; Lonetti et al., 2011).

Solubilized and non-solubilized samples that contained equivalent amounts of Vtc4 were used in synthesis assays. The linear phase of polyP synthesis allowed us to estimate the apparent turnover rate of the VTC complex in intact vacuoles, using a calibration curve measured with synthetic polyP-60 (Fig. 3A). PolyP accumulated at a rate of 0.21±0.02 nmol·µg^{-1}·min^{-1} (mean±s.e.m.), resulting in an apparent turnover rate of the VTC complex of k_{cat}^{app}= 220 min^{-1} (Fig. 6B).

Solubilization of vacuoles in CHAPS did not increase the turnover rate of the VTC complex but decreased it by a factor of ~20 (k_{cat}^{app}=10±1 min^{-1}). The remaining activity was not affected by concanamycin A or by FCCP (Fig. 6C), suggesting that these agents do not inhibit the catalytic activity of the VTC complex per se. These observations provide no indications that vacuolar proton pumping might support polyP synthesis through the import of counter-ions to compensate for possible charge transfer by polyP. The data are compatible with the view that the electrochemical gradient across the membrane is needed to actively support synthesis and translocation of the polyP chain and suggest that the VTC complex requires an intact and energized membrane environment in order to function efficiently.

Journal of Cell Science

Journal of Cell Science (2014) 127, 5093–5104 doi:10.1242/jcs.159772

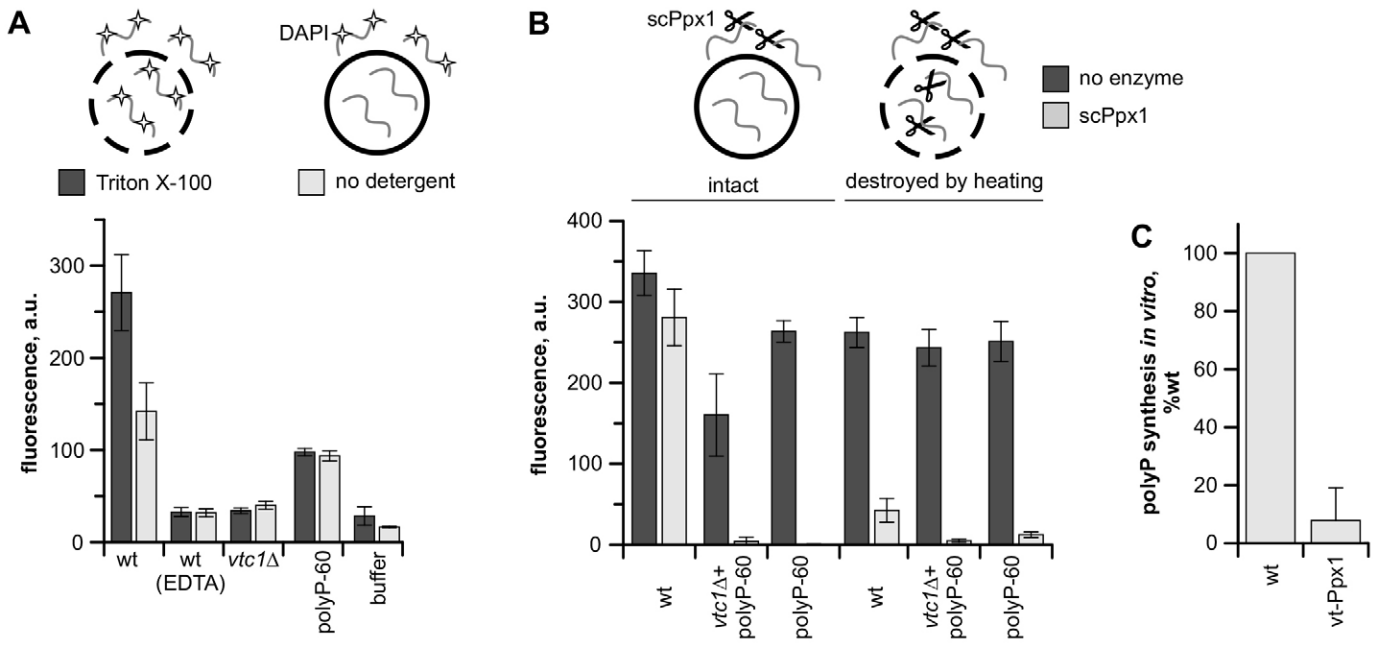

Fig. 4. Synthesized polyP is translocated into the vacuole lumen. (A,B) Vacuoles were isolated from BJ3505 wild-type (wt) or *vtc1*Δ cells, incubated with ATP-RS (30 min, 27˚C) and analyzed. (A) Accessibility of the synthesized polyP to DAPI. The reactions were stopped by adding EDTA and DAPI, and were split into two aliquots. One received Triton X-100, the other received control buffer. The polyP-60 sample contained 10 μM polyP-60 and no vacuoles. a.u., arbitrary units. (B) Accessibility of synthesized polyP to recombinant Ppx1. After incubation, the samples were split into two aliquots. One was diluted, chilled on ice and supplemented with 10 μM synthetic polyP-60 where indicated. The other was diluted, boiled for 5 min and supplemented with 10 μM synthetic polyP-60 where indicated. Half of each sample received Ppx1, the other half was left untreated. After 30 min on ice, digestion was stopped by adding EDTA, Triton X-100 and DAPI, and fluorescence was measured. The polyP-60 sample contained no vacuoles. (C) The effect of vacuole-targeted (vt)-Ppx1 on polyP synthesis. PolyP synthesis activity (60 min, 27˚C) was measured with vacuoles from wild-type cells (BJ3505) expressing vt-Ppx1 or an empty plasmid. Values of the sample without vt-Ppx1 were set to 100%. Data show the mean±s.d.

PolyP synthesis and translocation occur concomitantly

In such a scenario, translocation of the nascent chain might be necessary to permit continued synthesis by the catalytic domain. We tested this hypothesis further by substituting residues far away from the catalytic center, in the transmembrane domains that form a predicted transmembrane channel. If synthesis were obligatorily coupled to translocation, such mutations should interfere with synthesis. If synthesis and translocation were not coupled, synthesized but non-translocated polyP should accumulate outside the vacuoles. Substitution of basic residues in the transmembrane domains of the VTC complex, for example by the $vtc1^{K24E}$, $vtc1^{K24S}$ and $vtc1^{R31E}$ alleles, abolishes polyP accumulation *in vivo*, whereas $vtc1^{R98E}$ has little influence (Hothorn et al., 2009). However, the *in vivo* approach could not differentiate whether synthesis and translocation were impaired or whether synthesis continued and only translocation was blocked. In the latter case, the potent cytosolic polyphosphatase Ppx1 of yeast cells might degrade the non-translocated material and prevent its accumulation despite continuous synthesis. The *in vitro* synthesis reaction now allows us to detect non-translocated pools, as shown above. Therefore, we analyzed synthesis and translocation in Vtc1 point mutants. Vacuoles from $vtc1^{K24E}$,

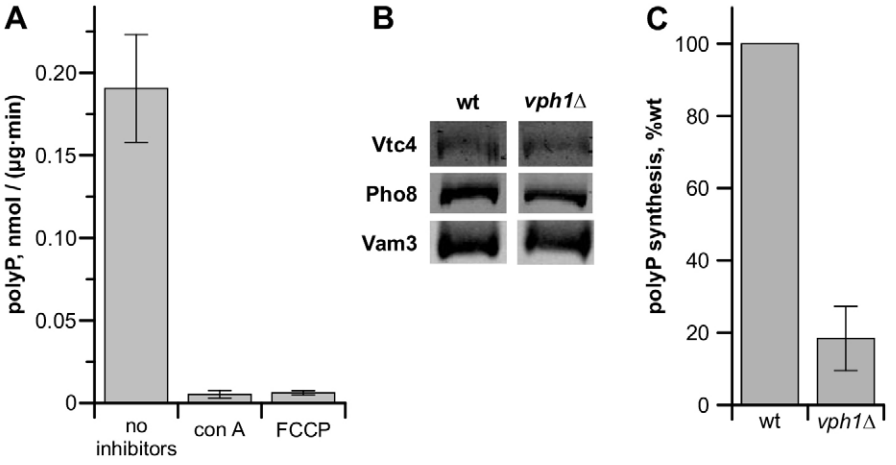

Fig. 5. Requirement of the vacuolar proton gradient for polyP synthesis by isolated vacuoles. (A) 1 μg of vacuoles from BY4742 *ppx1*Δ *ppn1*Δ cells was incubated for 10 min in the absence or presence of concanamycin A (1 μM) or FCCP (0.1 μM), and the amount of synthesized polyP was measured. (B,C) Vacuoles from wild-type (wt, BJ3505) and *vph1*Δ cells were isolated and (B) blotted for Vtc4, Pho8 and Vam3 or (C) assayed for *in vitro* polyP synthesis for 30 min at 27˚C. The amount of the synthesized polyP was determined by measuring DAPI–polyP fluorescence in the presence of Triton X-100. Data in A,C show the mean±s.d.

Journal of Cell Science

Journal of Cell Science (2014) 127, 5093–5104 doi:10.1242/jcs.159772

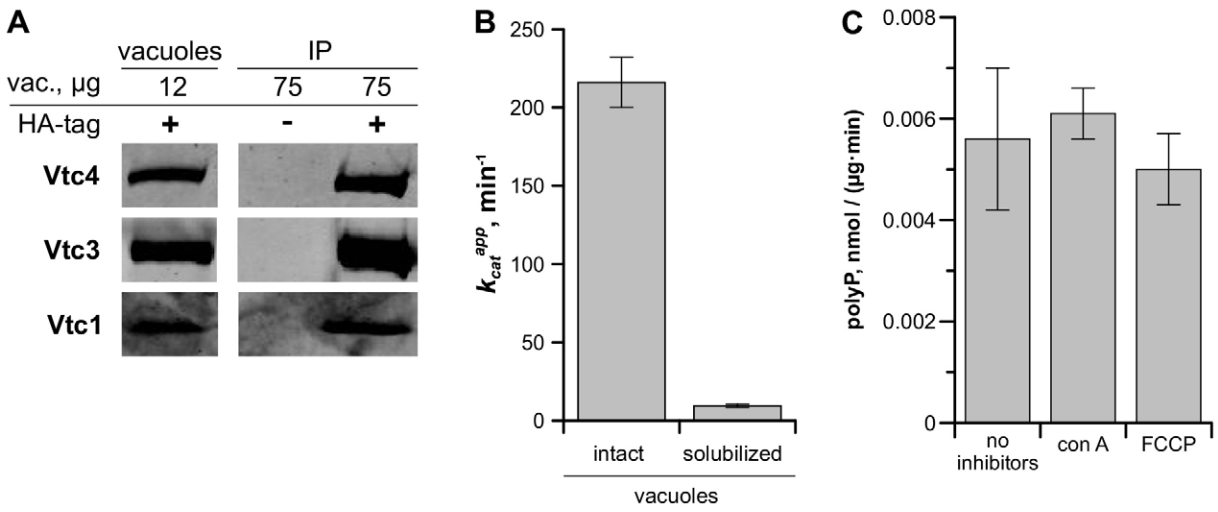

Fig. 6. PolyP synthesis by vacuole detergent extract. (A) Intactness of the VTC complex in detergent. Vacuoles (vac.) were isolated from BJ3505 Vtc3-3HA cells, solubilized in 15 mM CHAPS and immunoadsorbed to an anti-HA matrix. Adsorbed proteins were analyzed by SDS-PAGE and western blotting against the indicated proteins. IP, immunoprecipitated. (B) Catalytic activity after solubilization. Vacuoles from BY4742 *ppx1*Δ *ppn1*Δ were prepared and either left intact or solubilized in CHAPS. *In vitro* polyP synthesis activity was determined and the apparent catalytic turnover number was calculated. (C) Residual polyP synthesis activity in the detergent extract is insensitive to concanamycin A (con A) and FCCP. The vacuole detergent extracts were incubated with ATP-RS for 90 min without inhibitors, or with 1 µM concanamycin A or 0.1 µM FCCP, and the amount of synthesized polyP was measured. Data show the mean±s.d.

vtc1^{K24S} and *vtc1*^{R31E} cells did not accumulate polyP *in vitro* (Fig. 7A). *vtc1*^{R98E} supported polyP synthesis, albeit at a highly reduced rate. However, also in this mutant all the synthesized polyP was transferred into the vacuole lumen (Fig. 7B).

We also tested the capacity of isolated vacuoles to import synthetic polyP-60. This experiment addresses the question whether a potential free pool of polyP – if it existed – could be translocated or whether translocation might require a direct feeding of the nascent polyP chain from the catalytic domain into the translocation channel. During 10 min of the *in vitro* synthesis reaction, 2 µg of vacuoles translocated ≥1 nmol polyP into the lumen of the vacuole (Fig. 7C). If the VTC complex produced a soluble intermediate that was then imported, we would expect that soluble synthetic polyP-60 should also be importable at similar rates. We tested this hypothesis using vacuoles from strains lacking the vacuolar polyphosphatase Ppn1, which minimized the possibility that, whenever translocated, polyP-60 would be degraded in the lumen. We analyzed vacuoles from three strains – *ppn1*Δ vacuoles, providing the complete system with its ability to synthesize and translocate; *vtc4*^{R264A} *ppn1*Δ, containing a substitution of an active-site residue that renders the VTC complex catalytically inactive yet correctly assembled on the vacuole membrane (Hothorn et al., 2009); and *vtc4*Δ *ppn1*Δ, lacking the VTC complex. Vacuoles from these strains were incubated with 3 nmol polyP-60 in the presence of an ATP-regenerating system. After the incubation, the reactions were stopped by adding EDTA and DAPI, and the fractions of translocated and non-translocated polyP-60 were determined as established above (Fig. 7D). In all three cases no import of synthetic polyP-60 could be observed. Taken together, our observations suggest that efficient polyP synthesis requires concomitant translocation of the nascent chain into the vacuole and that polyP can only be efficiently imported as it emanates from the catalytic center of the VTC complex.

DISCUSSION

Given the toxicity of freely diffusible polyP and its exposure to the cytosolic polyphosphatase Ppx1, it appears plausible that synthesis of polyP should be coupled to its immediate translocation into the vacuole. Both *in vivo* and *in vitro* data support this hypothesis. *In vivo*, overexpression of Ppx1 in the cytosol does not affect polyP accumulation, whereas targeting Ppx1 into the vacuole lumen reduces polyP content dramatically. This argues that the cells do not accumulate a significant polyP pool in the cytosol. A further argument can be deduced from the similar toxicity of *Ec*Ppk1 expression in wild-type and *vtc1*Δ cells. Assuming a polyP translocase that transports freely diffusible polyP, we could explain the toxicity of *Ec*Ppk1 expression only if this translocase were saturated. Then, however, we could not explain why *Ec*Ppk1 induces similar polyP toxicity in *vtc1*Δ as in wild-type cells. *vtc1*Δ cells produce virtually no endogenous polyP and *Ec*Ppk1 establishes a polyP pool equivalent to only 20% of that seen in wild-type cells. In *vtc1*Δ cells, an independent translocase should thus have more than enough transport capacity to avoid toxicity and accumulation of cytosolic polyP. But this is not observed, suggesting that freely diffusible polyP might not be a substrate for translocation. This conclusion is strongly supported by the *in vitro* observation that isolated vacuoles efficiently import polyP produced by the VTC complex but not chemically synthesized polyP. Furthermore, inhibition of V-ATPase did not simply lead to accumulation of the synthesized polyP outside the vacuole, but blocked the entire reaction. We hence favor the interpretation that VTC acts as a coupled polyP polymerase and translocase. This could also explain the high number of transmembrane domains that are present in the VTC complex. VTC transmembrane domains contain conserved positively charged residues that are predicted to lie within the bilayer. These residues are far from the catalytic center and cannot even be expected to interact with the catalytic domain, but their substitution impairs polyP synthesis. This effect

Journal of Cell Science

Journal of Cell Science (2014) 127, 5093–5104 doi:10.1242/jcs.159772

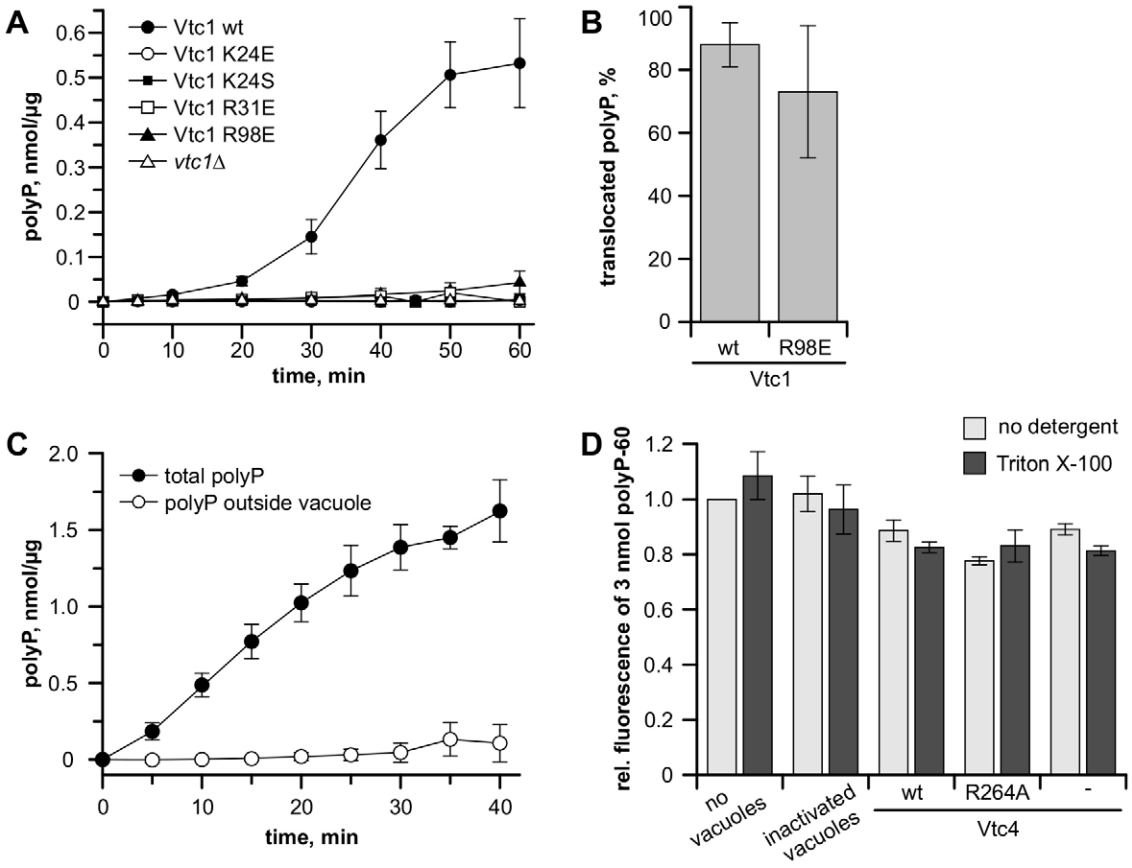

Fig. 7. PolyP synthesis and translocation are coupled. (A,B) *In vitro* synthesis reactions were run with 8 µg of vacuoles from BY4727 *vtc1Δ* cells reconstituted with the indicated mutant versions of VTC1. (A) Timecourse of polyP synthesis. (B) Translocation of the synthesized polyP by *vtc1*^{R98E} vacuoles, as measured by using the DAPI-accessibility assay. (C) Timecourse of polyP synthesis and translocation by 2 µg of vacuoles from BY4742 *ppn1*Δ *vtc4*Δ *VTC4*^{wt}, as measured by using the DAPI accessibility assay. (D) Translocation of synthetic polyP-60 by vacuoles. Vacuoles were isolated from BY4742 *ppn1*Δ *vtc4*Δ cells, reconstituted with the indicated versions of VTC4, and incubated with or without 3 nmol polyP-60 for 10 min under conditions used for the *in vitro* synthesis reaction. The amounts of polyP accessible to DAPI in the presence or absence of Triton X-100 were determined. Fluorescence of samples without polyP-60 was subtracted from the respective values with polyP-60. The fluorescence of 30 µM polyP-60 without vacuoles and without detergent was set to 1. The experiment was performed twice with two independent vacuole preparations, each in duplicates. Data show the mean±s.d. wt, vacuoles from wild-type cells.

is consistent with a coupling of synthesis and translocation. Structurally, such coupling is also plausible because the catalytic domain of the VTC complex forms a tunnel in which the catalytic reaction takes place. The polyP chain is held in the tunnel by interaction with numerous positively charged residues (Hothorn et al., 2009). It can be expected that the polyP chain must continuously slide forward in order to discharge the catalytic center and permit the addition of new phosphate residues, which could be facilitated by the concomitant translocation of the chain across the membrane. A remaining caveat is that polyP translocation into the vacuole lumen could be performed by a hypothetical independent polyP translocase, which might be downregulated in cells lacking functional VTC (*vtc1*Δ, *vtc4*Δ and *vtc4*^{R264A}).

How could polyP translocation be driven? PolyP synthesis itself could drive translocation. This is unlikely because the transfer of the γ-phosphate of a nucleotide triphosphate onto a polyP chain should be energetically almost neutral. But translocation and synthesis of polyP depend on the vacuolar electrochemical potential. A direct effect of the electrochemical potential on catalysis cannot be excluded, but we consider this to be equally unlikely, because the catalytic site is located in a separate cytosolic domain, i.e. outside the membrane. Several (not mutually exclusive) ways can be envisioned in which the electrochemical potential could support polyP translocation. Translocation might operate by a molecular ratchet (Feld et al., 2012), which exploits the spontaneous bidirectional Brownian motion of the polymer in the translocation channel. Selective binding of polyP at the lumenal face of the vacuolar membrane could impair back-sliding of the chain and make the process unidirectional. Suitable ligands that are known to bind to polyP are abundant in all acidocalcisomes, such as lysine, arginine, polyamines, Ca^{2+} and Mg^{2+} (Docampo and Moreno, 2011). Because the accumulation of these compounds inside vacuoles mostly depends on proton antiporters (Russnak et al., 2001; Tomitori et al., 2001; Shimazu et al., 2005; Brohée et al., 2010), the electrochemical potential could support polyP translocation by the import of these ligands into vacuoles. Protonation of polyP is unlikely to play a major role here, because the pH of vacuole lumen is 5.5 (Brett et al., 2011), whereas the sole hydroxyl group on each phosphate residue of polyP is strongly acidic (pK_a ~1–2) (Lee and Whitesides, 2010). A further hypothesis, which we favor, is that translocation is directly driven by the electrical potential across the vacuolar membrane. As a consequence of the

Journal of Cell Science

permanent pumping of protons into the vacuolar lumen, vacuoles show a membrane potential of 75 mV, positive inside (Kakinuma et al., 1981). PolyP, with its high density of negative charges, could be driven into vacuoles by this membrane potential. Interestingly, the polyP synthesis in *Dictyostelium discoideum* vacuoles, possibly acidocalcisomes, is inhibited by carbonyl cyanide *m*-chlorophenyl hydrazone (CCCP), suggesting that it might also depend on the proton gradient (Gómez-García and Kornberg, 2004). However, an opposite example also exists: polyP synthesis by the organelle fraction from arbuscular fungi was reported to be insensitive to CCCP (Tani et al., 2009). Therefore, it remains to be determined how universal is the requirement for the energized membrane environment for polyP synthesis in eukaryotes.

We found that the cytosolic production of polyP impairs the growth of yeast cells even if this production augmented polyP by only 10–20% of the amount normally found inside a wild-type cell. PolyP is probably sequestered in a specialized compartment and its synthesis coupled to translocation in order to avoid such cytosolic intermediates. This model can also rationalize the existence of the highly active cytosolic polyphosphatase Ppx1 (Wurst and Kornberg, 1994), which should cleave non-translocated polyP and protect cells against its adverse effects. In contrast to the toxic effects we found in yeast, a recent study in bacteria provided evidence for a protective, chaperone-like function of polyphosphates (Gray et al., 2014), which was proposed to augment bacterial stress resistance (Rao et al., 2009). Such a protective effect does not necessarily contradict the toxicity of polyP that we observed. PolyP showed beneficial effects on model proteins over a broad concentration range (from low micromolar to tens of millimolar). The presence of polyP in the cytosol might be regulated, restricting it to low concentrations. Here, it might be important that the major fraction of polyP is compartmentalized in volutin granules or acidocalcisome-like organelles even in bacteria (Seufferheld et al., 2003). PolyP might be released from these compartments into the cytosol if needed to survive stress conditions. It is conceivable that there could be a trade-off between the negative effects of transiently released higher concentrations of polyP on growth rate and its benefits for survival of the existing cells. This raises the interesting question of whether and how the production, translocation, turnover and potential release of polyP could be regulated in response to stress conditions.

Given that the sequestration of polyP in compartments is a universal feature, we expect that the protective as well as the toxic aspects of polyP metabolism will be of broad relevance for eukaryotic as well as prokaryotic organisms. Therefore, the biogenesis and metabolism of acidocalcisomes and of the polyphosphates stored in them should be further explored.

MATERIALS AND METHODS

Materials

Creatine kinase, creatine phosphate and ATP were from Roche, concanamycin A was from Alexis. PolyP-60 and polyP-300 were kind gifts from Toshikazu Shiba (Regenetiss Inc., Japan). The concentration of polyP was verified by an enzymatic assay (Hothorn et al., 2009) and is reported as the concentration of phosphate monomers. Anti-HA monoclonal mouse antibody HA.11 was from Covance. Polyclonal antibodies were raised in rabbits using proteins expressed in *E. coli*.

Yeast strains and plasmids

Strains are listed in supplementary material Table S1. Genes were deleted by replacing a complete open reading frame with a marker cassette (Janke et al., 2004; see supplementary material Table S2 for PCR primers). BY4742 *ppx1*Δ *ppn1*Δ was constructed from BY4742 *ppn1*Δ::kanMX (Euroscarf; accession number Y14286). BY4742 *vtc4*Δ *ppn1*Δ and BY4742 *vtc4*Δ *ppn1*Δ VTC^{R264X} were constructed from BY4742 *vtc4*Δ (Euroscarf; accession number Y16780) and BY4742 *vtc4*Δ $VTC4^{R264X}$ (Hothorn et al., 2009), respectively. BJ3505 Vtc3-6gly-3HA was generated by genomic integration of a PCR fragment coding for the tag and the auxotrophic marker using the pUG6 plasmid (Güldener et al., 1996). BY4741 P_{GAL}-3HA-PPX1 was produced by PCR-based tagging (Janke et al., 2004). The tag was amplified from the plasmid pYMN-24, the PCR product was integrated into BY4741 and clones were selected on nourseothricin-containing plates. Two positive clones were selected and transformed either with $p416_{GPD}$ or $p416_{GPD}$PPK1. Clones were selected on plates containing 2% galactose in place of glucose ($HC^{-URA+GAL}$). Genomic manipulations were verified by colony PCR.

Genomic DNA from *S. cerevisiae* BY4741 and *E. coli* TOP10 was extracted using the Gentra Puregen Yeast/Bacteria Kit (Qiagen). The coding sequences of yeast Ppx1, *Ec*Ppk1 and the pre-pro-sequence of yeast CPY (PPCPY), consisting of sequence encoding 111 N-terminal amino acids, were amplified by PCR from genomic DNA using primers described in supplementary material Table S2. For the expression of vacuole-targeted Ppx1, PPCPY was digested by using *Bam*HI and *Eco*RI and cloned into the $p416_{GPD}$ plasmid (ATCC number 87360), giving plasmid $p416_{GPD}$PPCPY. The *PPX1* ORF was digested by using *Eco*RI and *Xho*I and cloned into pYD010, giving plasmid $p416_{GPD}$PPCPY-Ppx1. To construct the plasmid encoding Ppx1–GFP, we first amplified the *PPX1* ORF lacking the stop codon from genomic yeast DNA and digested the product using *Eco*RI and *Xho*I. The insert was ligated with $p416_{GPD}$PPCPY, giving $p416_{GPD}$PPCPY-Ppx1minusSTOP. GFP was then amplified from plasmid pKT127 and the PCR product was digested using *Xho*I and *Mlu*I before ligation with $p416_{GPD}$PPCPY-Ppx1minusSTOP to give $p416_{GPD}$PPCPY-Ppx1-GFP. For cytosolic expression of Ppx1, the coding sequence of *PPX1* was PCR-amplified, digested with *Eco*RI and *Hind*III and cloned into $p416_{GPD}$, giving plasmid $p416_{GPD}$Ppx1. For the cytosolic expression of *Ec*Ppk1, the coding sequence of *PPK1* was amplified, digested by using *Hind*III and *Xho*I and the product was inserted into $p416_{GPD}$, giving plasmid $p416_{GPD}$PPK1. Plasmids were sequenced (Fasteris).

Purification of recombinant ScPPX1

E.coli BL21 cells were transformed with the plasmid pKM263*ScPPX1* (Werner et al., 2005), grown in 2 l of NZ-medium (10 g/l yeast extract, 2 g/l glucose, 5 g/l NaCl, 16 g/l NZ-amine, 100 g/l ampicillin) at 30℃ to an OD_{600} of 1, shifted to 20℃ and incubated overnight. Cells were harvested and resuspended in 30 ml of cold lysis buffer (50 mM Tris-HCl pH 7.5, 300 mM NaCl, 20 mM imidazole) and 1 mg/ml lysozyme was added for 30 min at 4℃, followed by six sonication steps of 15 s. 10 µg/ml RNase (Applichem) and 5 µg/ml DNase (Roche) were added, and the incubation was continued for 30 min at 0℃. The lysate was centrifuged (30 min, 66,000 ***g***, 4℃) and supernatant (35 ml) was loaded onto a column containing 2.2 ml of Protino^{R}Ni-Ted resin (Macherey-Nagel) pre-equilibrated in lysis buffer. Beads were washed with 40 ml of cold lysis buffer and eluted with 9 ml of cold elution buffer 1 (50 mM Tris-HCl pH 7.5, 300 mM NaCl, 200 mM imidazole). Elution fractions were loaded on a column containing 2 ml of glutathione Sepharose^{TM} (GE Healthcare) pre-equilibrated in cold elution buffer 1. After washing with 30 ml of cold elution buffer 1, proteins were eluted with 6 ml of cold elution buffer 2 (50 mM Tris-HCl pH 7.5, 10% sucrose, 10 mM glutathione) and dialysed against 4 l of 50 mM Tris-HCl pH 7.5, 10% sucrose overnight at 4℃. Protein concentration was determined by the Bradford assay (BioRad) using bovine serum albumin (BSA) as the standard.

Media and growth of cells

Precultures were prepared in YPD or, for the strains carrying $p416_{GPD}$-derived plasmids, in Hartwell's complete medium without uracil (HC^{-URA}) (Burke et al., 2000) and grown at 30℃ for 24–48 h. An appropriate amount of cells were inoculated into the fresh medium,

grown overnight at 30℃ until an OD_{600} of 1–2 was reached and used for further experiments. In $HC^{-URA+GAL}$ medium 2% glucose was replaced with 2% galactose.

Isolation and solubilization of vacuoles

The cells were grown in 1 litre of YPD medium at 30℃ overnight and harvested at an OD_{600} of 0.6–1.3. A total of 600 ml of culture was centrifuged (2 min, 3900 ***g***), cells were resuspended in 50 ml of 0.1 M Tris-HCl pH 8.9, 10 mM DTT, incubated for 7 min at 30℃ in a water bath and collected by centrifugation. Cells were resuspended in 15 ml of spheroplasting buffer (50 mM potassium phosphate pH 7.5, 600 mM sorbitol in YPD with 0.2% glucose), 3000–4500 units of lyticase (Cabrera and Ungermann, 2008) were added and cells were incubated for 26 min at 30℃ in a water bath. Spheroplasts were collected by centrifugation (3 min, 3400 ***g***, 4℃) and gently resuspended in 15 ml of 15% Ficoll 400 in PS buffer (10 mM PIPES/KOH pH 6.8, 200 mM sorbitol). Spheroplasts were lysed by adding DEAE-dextran to a concentration of 7 mg/l and incubated (2 min, 0℃, then 2 min, 30℃). Samples were chilled, transferred into SW41 tubes and overlaid with 2.5 ml of 8% Ficoll 400, 3.5 ml of 4% Ficoll 400, and 1.5 ml of 0% Ficoll 400 (all in PS buffer). After centrifugation (150,000 ***g***, 90 min, 4℃), vacuoles were harvested from the 0–4% interface. When isolating vacuoles from proteolytically competent strains, 1 mM PMSF and 1× protease inhibitor cocktail (1× PIC – 100 µM pefabloc SC, 100 ng/ml leupeptin, 50 µM *O*-phenanthroline and 500 ng/ml pepstatin A) were included in all buffers, starting from the spheroplasting step. Vacuole amounts were determined by protein content, using the Bradford assay with fatty-acid-free BSA as standard. Individual proteins on isolated vacuoles were analyzed by SDS-PAGE and western blotting. Secondary antibodies were coupled to IR dyes and the bands of interest were quantified using the Odyssey software (V1.1) (LI-COR).

Detergent extracts of vacuoles were prepared as follows: vacuoles in PS buffer were supplemented with 2% DMSO, frozen in liquid nitrogen and stored at −20℃. Before use, they were thawed on ice, pelleted (7000 ***g***, 5 min, 4℃) and resuspended in 20 mM potassium phosphate buffer pH 7.5, 150 mM KCl, 0.5 mM $MnCl_2$, 1× PIC, 1 mM PMSF and 15 mM CHAPS and incubated on ice for 20–45 min with occasional mixing. Insoluble material was removed by centrifugation (20,000 ***g***, 15 min, 4℃).

PolyP synthesis by isolated vacuoles

PolyP synthesis was assayed in 100-µl samples consisting of reaction buffer (10 mM PIPES/KOH pH 6.8, 150 mM KCl, 0.5 mM $MnCl_2$, 200 mM sorbitol) and ATP-regenerating system (ATP-RS – 1 mM ATP-$MgCl_2$, 40 mM creatine phosphate and 0.25 mg/ml creatine kinase). The reactions were started by adding 2 µg of purified vacuoles, the samples were incubated at 27℃, followed by addition of 200 µl of stop solution (12 mM EDTA, 0.15% Triton X-100 and 15 µM DAPI) in dilution buffer (10 mM PIPES/KOH pH 6.8, 150 mM KCl, 200 mM sorbitol). This threefold dilution with EDTA-containing buffer did not only stop nucleotide hydrolysis but also resulted in faster development of DAPI–polyP fluorescence. Given that DAPI is membrane impermeable, dissolving the membranes with detergent was required in order to detect the entire polyP pool. A total of 240 µl of the sample was transferred into a black 96-well plate and fluorescence was measured with a SPECTRAmax GEMINI XS fluorescence plate reader (Molecular Devices) using λ_{ex}=415 nm, λ_{em}=550 nm (cutoff=530 nm) at 27℃. Fluorescence was read every 1–2 min until the signal was stable. Experiments were repeated with at least three independent vacuole preparations. Values are presented as the mean±s.d. In case of vacuole detergent extracts, polyP synthesis was performed in the same buffer as solubilisation, in the presence of CHAPS.

Accessibility of the synthesized polyP to DAPI staining

4 µg of BJ3505 vacuoles were incubated in 200 µl of reaction buffer with ATP-RS for 30 min at 27℃. Then, 400 µl of ice-cold stop solution without Triton X-100 was added, the samples were vortexed briefly and a 250-µl aliquot was transferred into a black clear-bottomed 96-well plate ('no detergent' sample). The rest of the sample was immediately supplemented with 0.1% Triton X-100 (final concentration), vortexed vigorously and a second 250-µl aliquot was withdrawn ('+ detergent' sample). DAPI–polyP fluorescence was measured with a SPECTRAmax GEMINI EM fluorescence plate reader in a bottom-reading mode in order to avoid detergent artifacts related to meniscus curvature (Cottingham et al., 2004; Lifeng and Gochin, 2007).

Accessibility of the synthesized polyP to recombinant Ppx1

16 µg of BJ3505 vacuoles were incubated in 800 µl of reaction buffer with ATP-RS for 30 min at 27℃. A control sample was incubated in the presence of 8 mM EDTA. After chilling on ice, 10 µM polyP-60 standard (final concentration) was added to *vtc1*Δ and 'no vacuole' samples. Two 100-µl aliquots were withdrawn, mixed with 200 µl of dilution buffer and incubated on ice with or without 0.2 µg of recombinant Ppx1 for 30 min. 8 mM EDTA, 0.1% Triton X-100 and 10 µM DAPI were added and DAPI–polyP fluorescence was measured.

400 µl of the remaining reaction mixtures were mixed with 800 µl of dilution buffer that had been pre-heated to 99℃, boiled for 5 min and placed on ice. Two 300-µl aliquots were incubated with or without recombinant Ppx1 as described above for the untreated samples. 250 µl was transferred into a 96-well plate and DAPI–polyP fluorescence was measured (see above). To correct for polyP-unrelated fluorescence, background values were subtracted. For BJ3505 vacuoles, the sample incubated with EDTA was used for background correction; in case of BJ3505 *vtc1*Δ vacuoles and 'no vacuoles' samples, reactions without added polyP-60 served as background values.

Quantification of polyP accumulated *in vivo*

PolyP was extracted, purified on Qiagen PCR purification columns and digested with recombinant Ppx1, and the released orthophosphate was quantified by using a colorimetric assay with Malachite Green as described previously (Hothorn et al., 2009). Experiments were performed at least in duplicates for at least two different transformants. The results are presented as the mean±s.d.

Microscopy

For observation of cell morphology and localization of vtGFP–Ppx1, the cells were grown in HC^{-URA} to an OD_{600} of 1.0, collected by centrifugation and mounted on a microscopy slide. For the quantification of viable cells, the cells were resuspended in 10 mM HEPES pH 7.5 containing 2% glucose, 20 µM of FUN1 was added and samples were incubated for 30 min at 30℃ in the dark. Aliquots were observed using a LEICA DMI6000 B microscope with a 100× 1.4 NA lens, a Hamamatsu ORCA-R2 camera and an X-Cite® series 120Q UV lamp. Pictures were collected using Volocity software (Perkin Elmer) and treated with ImageJ software. Living cells were counted in cultures of at least two transformants.

Acknowledgements

We thank Toshikazu Shiba (Regenetiss Inc., Japan) for synthetic polyP-60 and polyP-300 and Adolfo Saiardi (London, UK) for the introduction into electrophoresis of polyphosphates.

Competing interests

The authors declare no competing interests.

Author contributions

A.M. conceived of the general idea. R.G., S.S., Y.D. and A.S. designed and performed the experiments. R.G., S.S., Y.D. and A.M. analyzed the results and wrote the manuscript.

Funding

This work was supported by grants from the Swiss National Science Foundation; and European Research Council to A.M.

Supplementary material

Supplementary material available online at
http://jcs.biologists.org/lookup/suppl/doi:10.1242/jcs.159772/-/DC1

Journal of Cell Science

References

Ahn, K. and Kornberg, A. (1990). Polyphosphate kinase from Escherichia coli. Purification and demonstration of a phosphoenzyme intermediate. *J. Biol. Chem.* **265**, 11734-11739.

Akiyama, M., Crooke, E. and Kornberg, A. (1992). The polyphosphate kinase gene of Escherichia coli. Isolation and sequence of the ppk gene and membrane location of the protein. *J. Biol. Chem.* **267**, 22556-22561.

Aschar-Sobbi, R., Abramov, A. Y., Diao, C., Kargacin, M. E., Kargacin, G. J., French, R. J. and Pavlov, E. (2008). High sensitivity, quantitative measurements of polyphosphate using a new DAPI-based approach. *J. Fluoresc.* **18**, 859-866.

Auesukaree, C., Homma, T., Tochio, H., Shirakawa, M., Kaneko, Y. and Harashima, S. (2004). Intracellular phosphate serves as a signal for the regulation of the PHO pathway in Saccharomyces cerevisiae. *J. Biol. Chem.* **279**, 17289-17294.

Bayer, M. J., Reese, C., Buhler, S., Peters, C. and Mayer, A. (2003). Vacuole membrane fusion: V0 functions after trans-SNARE pairing and is coupled to the Ca2+-releasing channel. *J. Cell Biol.* **162**, 211-222.

Besteiro, S., Tonn, D., Tetley, L., Coombs, G. H. and Mottram, J. C. (2008). The AP3 adaptor is involved in the transport of membrane proteins to acidocalcisomes of Leishmania. *J. Cell Sci.* **121**, 561-570.

Bolesch, D. G. and Keasling, J. D. (2000). Polyphosphate binding and chain length recognition of Escherichia coli exopolyphosphatase. *J. Biol. Chem.* **275**, 33814-33819.

Baker Brachmann, C., Davies, A., Cost, G. J., Caputo, E., Li, J., Hieter, P. and Boeke, J. D. (1998). Designer deletion strains derived from Saccharomyces cerevisiae S288C: a useful set of strains and plasmids for PCR-mediated gene disruption and other applications. *Yeast* **14**, 115-132.

Brett, C. L., Kallay, L., Hua, Z., Green, R., Chyou, A., Zhang, Y., Graham, T. R., Donowitz, M. and Rao, R. (2011). Genome-wide analysis reveals the vacuolar pH-stat of Saccharomyces cerevisiae. *PLoS ONE* **6**, e17619.

Brohée, S., Barriot, R., Moreau, Y. and André, B. (2010). YTPdb: a wiki database of yeast membrane transporters. *Biochim. Biophys. Acta* **1798**, 1908-1912.

Burke, D., Dawson, D., Stearns, T. and Laboratory, C. S. H. (2000). *Methods in Yeast Genetics: A Cold Spring Harbor Laboratory Course Manual*. Cold Spring Harbor, NY: Cold Spring Harbor Laboratory Press.

Cabrera, M. and Ungermann, C. (2008). Purification and in vitro analysis of yeast vacuoles. *Methods Enzymol.* **451**, 177-196.

Chen, W., Palmer, R. J. and Kuramitsu, H. K. (2002). Role of polyphosphate kinase in biofilm formation by Porphyromonas gingivalis. *Infect. Immun.* **70**, 4708-4715.

Choi, S. H., Smith, S. A. and Morrissey, J. H. (2011). Polyphosphate is a cofactor for the activation of factor XI by thrombin. *Blood* **118**, 6963-6970.

Cottingham, M. G., Bain, C. D. and Vaux, D. J. (2004). Rapid method for measurement of surface tension in multiwell plates. *Lab. Invest.* **84**, 523-529.

de Jesus, T. C., Tonelli, R. R., Nardelli, S. C., da Silva Augusto, L., Motta, M. C., Girard-Dias, W., Miranda, K., Ulrich, P., Jimenez, V., Barquilla, A. et al. (2010). Target of rapamycin (TOR)-like 1 kinase is involved in the control of polyphosphate levels and acidocalcisome maintenance in Trypanosoma brucei. *J. Biol. Chem.* **285**, 24131-24140.

Diaz, J. M. and Ingall, E. D. (2010). Fluorometric quantification of natural inorganic polyphosphate. *Environ. Sci. Technol.* **44**, 4665-4671.

Docampo, R. and Moreno, S. N. (2011). Acidocalcisomes. *Cell Calcium* **50**, 113-119.

Docampo, R., de Souza, W., Miranda, K., Rohloff, P. and Moreno, S. N. (2005). Acidocalcisomes - conserved from bacteria to man. *Nat. Rev. Microbiol.* **3**, 251-261.

Docampo, R., Ulrich, P. and Moreno, S. N. (2010). Evolution of acidocalcisomes and their role in polyphosphate storage and osmoregulation in eukaryotic microbes. *Philos. Trans. R. Soc. B* **365**, 775-784.

Fang, J., Rohloff, P., Miranda, K. and Docampo, R. (2007). Ablation of a small transmembrane protein of Trypanosoma brucei (TbVTC1) involved in the synthesis of polyphosphate alters acidocalcisome biogenesis and function, and leads to a cytokinesis defect. *Biochem. J.* **407**, 161-170.

Feld, G. K., Brown, M. J. and Krantz, B. A. (2012). Ratcheting up protein translocation with anthrax toxin. *Protein Sci.* **21**, 606-624.

Freimoser, F. M., Hürlimann, H. C., Jakob, C. A., Werner, T. P. and Amrhein, N. (2006). Systematic screening of polyphosphate (poly P) levels in yeast mutant cells reveals strong interdependence with primary metabolism. *Genome Biol.* **7**, R109.

Gómez-García, M. R. and Kornberg, A. (2004). Formation of an actin-like filament concurrent with the enzymatic synthesis of inorganic polyphosphate. *Proc. Natl. Acad. Sci. USA* **101**, 15876-15880.

Gray, M. J., Wholey, W. Y., Wagner, N. O., Cremers, C. M., Mueller-Schickert, A., Hock, N. T., Krieger, A. G., Smith, E. M., Bender, R. A., Bardwell, J. C. et al. (2014). Polyphosphate is a primordial chaperone. *Mol. Cell* **53**, 689-699.

Güldener, U., Heck, S., Fielder, T., Beinhauer, J. and Hegemann, J. H. (1996). A new efficient gene disruption cassette for repeated use in budding yeast. *Nucleic Acids Res.* **24**, 2519-2524.

Hernandez-Ruiz, L., González-García, I., Castro, C., Brieva, J. A. and Ruiz, F. A. (2006). Inorganic polyphosphate and specific induction of apoptosis in human plasma cells. *Haematologica* **91**, 1180-1186.

Hoac, B., Kiffer-Moreira, T., Millán, J. L. and McKee, M. D. (2013). Polyphosphates inhibit extracellular matrix mineralization in MC3T3-E1 osteoblast cultures. *Bone* **53**, 478-486.

Holmström, K. M., Marina, N., Baev, A. Y., Wood, N. W., Gourine, A. V. and Abramov, A. Y. (2013). Signalling properties of inorganic polyphosphate in the mammalian brain. *Nat. Commun.* **4**, 1362.

Hothorn, M., Neumann, H., Lenherr, E. D., Wehner, M., Rybin, V., Hassa, P. O., Uttenweiler, A., Reinhardt, M., Schmidt, A., Seiler, J. et al. (2009). Catalytic core of a membrane-associated eukaryotic polyphosphate polymerase. *Science* **324**, 513-516.

Huang, G., Fang, J., Sant'Anna, C., Li, Z. H., Wellems, D. L., Rohloff, P. and Docampo, R. (2011). Adaptor protein-3 (AP-3) complex mediates the biogenesis of acidocalcisomes and is essential for growth and virulence of Trypanosoma brucei. *J. Biol. Chem.* **286**, 36619-36630.

Huang, G., Bartlett, P. J., Thomas, A. P., Moreno, S. N. and Docampo, R. (2013). Acidocalcisomes of Trypanosoma brucei have an inositol 1,4,5-trisphosphate receptor that is required for growth and infectivity. *Proc. Natl. Acad. Sci. USA* **110**, 1887-1892.

Indge, K. J. (1968). Polyphosphates of the yeast cell vacuole. *J. Gen. Microbiol.* **51**, 447-455.

Janke, C., Magiera, M. M., Rathfelder, N., Taxis, C., Reber, S., Maekawa, H., Moreno-Borchart, A., Doenges, G., Schwob, E., Schiebel, E. et al. (2004). A versatile toolbox for PCR-based tagging of yeast genes: new fluorescent proteins, more markers and promoter substitution cassettes. *Yeast* **21**, 947-962.

Jimenez-Nunez, M. D., Moreno-Sanchez, D., Hernandez-Ruiz, L., Benitez-Rondan, A., Ramos-Amaya, A., Rodriguez-Bayona, B., Medina, F., Brieva, J. A. and Ruiz, F. A. (2012). Myeloma cells contain high levels of inorganic polyphosphate which is associated with nucleolar transcription. *Haematologica* **97**, 1264-1271.

Jones, E. W., Zubenko, G. S. and Parker, R. R. (1982). PEP4 gene function is required for expression of several vacuolar hydrolases in Saccharomyces cerevisiae. *Genetics* **102**, 665-677.

Kakinuma, Y., Ohsumi, Y. and Anraku, Y. (1981). Properties of H+-translocating adenosine triphosphatase in vacuolar membranes of Saccharomyces cerevisiae. *J. Biol. Chem.* **256**, 10859-10863.

Kapuscinski, J. (1990). Interactions of nucleic acids with fluorescent dyes: spectral properties of condensed complexes. *J. Histochem. Cytochem.* **38**, 1323-1329.

Kim, K. S., Rao, N. N., Fraley, C. D. and Kornberg, A. (2002). Inorganic polyphosphate is essential for long-term survival and virulence factors in Shigella and Salmonella spp. *Proc. Natl. Acad. Sci. USA* **99**, 7675-7680.

Kuroda, A., Nomura, K., Ohtomo, R., Kato, J., Ikeda, T., Takiguchi, N., Ohtake, H. and Kornberg, A. (2001). Role of inorganic polyphosphate in promoting ribosomal protein degradation by the Lon protease in E. coli. *Science* **293**, 705-708.

Lander, N., Ulrich, P. N. and Docampo, R. (2013). Trypanosoma brucei vacuolar transporter chaperone 4 (TbVtc4) is an acidocalcisome polyphosphate kinase required for in vivo infection. *J. Biol. Chem.* **288**, 34205-34216.

Lee, A. and Whitesides, G. M. (2010). Analysis of inorganic polyphosphates by capillary gel electrophoresis. *Anal. Chem.* **82**, 6838-6846.

Lifeng, C. and Gochin, M. (2007). Colloidal aggregate detection by rapid fluorescence measurement of liquid surface curvature changes in multiwell plates. *J. Biomol. Screen.* **12**, 966-971.

Lonetti, A., Szijgyarto, Z., Bosch, D., Loss, O., Azevedo, C. and Saiardi, A. (2011). Identification of an evolutionarily conserved family of inorganic polyphosphate endopolyphosphatases. *J. Biol. Chem.* **286**, 31966-31974.

Madeira da Silva, L. and Beverley, S. M. (2010). Expansion of the target of rapamycin (TOR) kinase family and function in Leishmania shows that TOR3 is required for acidocalcisome biogenesis and animal infectivity. *Proc. Natl. Acad. Sci. USA* **107**, 11965-11970.

Martin, P. and Van Mooy, B. A. (2013). Fluorometric quantification of polyphosphate in environmental plankton samples: extraction protocols, matrix effects, and nucleic acid interference. *Appl. Environ. Microbiol.* **79**, 273-281.

Müller, O., Bayer, M. J., Peters, C., Andersen, J. S., Mann, M. and Mayer, A. (2002). The Vtc proteins in vacuole fusion: coupling NSF activity to V(0) trans-complex formation. *EMBO J.* **21**, 259-269.

Müller, O., Neumann, H., Bayer, M. J. and Mayer, A. (2003). Role of the Vtc proteins in V-ATPase stability and membrane trafficking. *J. Cell Sci.* **116**, 1107-1115.

Omelon, S. and Grynpas, M. (2011). Polyphosphates affect biological apatite nucleation. *Cells Tissues Organs* **194**, 171-175.

Pavlov, E., Aschar-Sobbi, R., Campanella, M., Turner, R. J., Gómez-García, M. R. and Abramov, A. Y. (2010). Inorganic polyphosphate and energy metabolism in mammalian cells. *J. Biol. Chem.* **285**, 9420-9428.

Perzov, N., Padler-Karavani, V., Nelson, H. and Nelson, N. (2002). Characterization of yeast V-ATPase mutants lacking Vph1p or Stv1p and the effect on endocytosis. *J. Exp. Biol.* **205**, 1209-1219.

Rao, N. N., Gómez-García, M. R. and Kornberg, A. (2009). Inorganic polyphosphate: essential for growth and survival. *Annu. Rev. Biochem.* **78**, 605-647.

Reusch, R. N. (1989). Poly-beta-hydroxybutyrate/calcium polyphosphate complexes in eukaryotic membranes. *Proc. Soc. Exp. Biol. Med.* **191**, 377-381.

Rooney, P. J., Ayong, L., Tobin, C. M., Moreno, S. N. and Knoll, L. J. (2011). TgVTC2 is involved in polyphosphate accumulation in Toxoplasma gondii. *Mol. Biochem. Parasitol.* **176**, 121-126.

Russnak, R., Konczal, D. and McIntire, S. L. (2001). A family of yeast proteins mediating bidirectional vacuolar amino acid transport. *J. Biol. Chem.* **276**, 23849-23857.

Saito, K., Ohtomo, R., Kuga-Uetake, Y., Aono, T. and Saito, M. (2005). Direct labeling of polyphosphate at the ultrastructural level in Saccharomyces cerevisiae by using the affinity of the polyphosphate binding domain of Escherichia coli exopolyphosphatase. *Appl. Environ. Microbiol.* **71**, 5692-5701.
Sethuraman, A., Rao, N. N. and Kornberg, A. (2001). The endopolyphosphatase gene: essential in Saccharomyces cerevisiae. *Proc. Natl. Acad. Sci. USA* **98**, 8542-8547.
Seufferheld, M., Vieira, M. C., Ruiz, F. A., Rodrigues, C. O., Moreno, S. N. and Docampo, R. (2003). Identification of organelles in bacteria similar to acidocalcisomes of unicellular eukaryotes. *J. Biol. Chem.* **278**, 29971-29978.
Shi, X. and Kornberg, A. (2005). Endopolyphosphatase in Saccharomyces cerevisiae undergoes post-translational activations to produce short-chain polyphosphates. *FEBS Lett.* **579**, 2014-2018.
Shimazu, M., Sekito, T., Akiyama, K., Ohsumi, Y. and Kakinuma, Y. (2005). A family of basic amino acid transporters of the vacuolar membrane from Saccharomyces cerevisiae. *J. Biol. Chem.* **280**, 4851-4857.
Smith, S. A. and Morrissey, J. H. (2007). Sensitive fluorescence detection of polyphosphate in polyacrylamide gels using 4′,6-diamidino-2-phenylindol. *Electrophoresis* **28**, 3461-3465.
Smith, S. A., Mutch, N. J., Baskar, D., Rohloff, P., Docampo, R. and Morrissey, J. H. (2006). Polyphosphate modulates blood coagulation and fibrinolysis. *Proc. Natl. Acad. Sci. USA* **103**, 903-908.
Stotz, S. C., Scott, L. O., Drummond-Main, C., Avchalumov, Y., Girotto, F., Davidsen, J., Gómez-Gárcia, M. R., Rho, J. M., Pavlov, E. V. and Colicos, M. A. (2014). Inorganic polyphosphate regulates neuronal excitability through modulation of voltage-gated channels. *Mol. Brain* **7**, 42.
Tani, C., Ohtomo, R., Osaki, M., Kuga, Y. and Ezawa, T. (2009). ATP-dependent but proton gradient-independent polyphosphate-synthesizing activity in extraradical hyphae of an arbuscular mycorrhizal fungus. *Appl. Environ. Microbiol.* **75**, 7044-7050.
Tomitori, H., Kashiwagi, K., Asakawa, T., Kakinuma, Y., Michael, A. J. and Igarashi, K. (2001). Multiple polyamine transport systems on the vacuolar membrane in yeast. *Biochem. J.* **353**, 681-688.
Urech, K., Dürr, M., Boller, T., Wiemken, A. and Schwencke, J. (1978). Localization of polyphosphate in vacuoles of Saccharomyces cerevisiae. *Arch. Microbiol.* **116**, 275-278.
Uttenweiler, A., Schwarz, H., Neumann, H. and Mayer, A. (2007). The vacuolar transporter chaperone (VTC) complex is required for microautophagy. *Mol. Biol. Cell* **18**, 166-175.
Werner, T. P., Amrhein, N. and Freimoser, F. M. (2005). Novel method for the quantification of inorganic polyphosphate (iPoP) in Saccharomyces cerevisiae shows dependence of iPoP content on the growth phase. *Arch. Microbiol.* **184**, 129-136.
Wurst, H. and Kornberg, A. (1994). A soluble exopolyphosphatase of Saccharomyces cerevisiae. Purification and characterization. *J. Biol. Chem.* **269**, 10996-11001.
Wurst, H., Shiba, T. and Kornberg, A. (1995). The gene for a major exopolyphosphatase of Saccharomyces cerevisiae. *J. Bacteriol.* **177**, 898-906.
Zhang, H., Gómez-García, M. R., Shi, X., Rao, N. N. and Kornberg, A. (2007). Polyphosphate kinase 1, a conserved bacterial enzyme, in a eukaryote, Dictyostelium discoideum, with a role in cytokinesis. *Proc. Natl. Acad. Sci. USA* **104**, 16486-16491.

Table S1. Yeast strains used in this study

Strain	Genotype	Source / Reference
BJ3505	MATa pep4::HIS3 prb1- Δ1.6R lys2-208 trp-Δ101 ura3-52 gal2 can	(Jones et al., 1982)
BJ3505 *vtc1*Δ	BJ3505, vtc1::kanMX	this study
BJ3505 *Ec*Ppk1	BJ3505, $p416_{GPD}$-*Ec*Ppk1	this study
BJ3505 *vtc1*Δ *Ec*Ppk1	BJ3505, vtc1::kanMX, $p416_{GPD}$-*Ec*PPK1	this study
BJ3505 Ppx1	BJ3505, $p416_{GPD}$-Ppx1	this study
BJ3505 vt-Ppx1	BJ3505, $p416_{GPD}$PPCPY-Ppx1	this study
BJ3505 vtGFP-Ppx1	BJ3505, $p416_{GPD}$PPCPY-Ppx1-GFP	this study
BJ3505 *vph1*Δ	BJ3505, vph1::kanMX	(Bayer et al., 2003)
BJ3505 Vtc3-3HA	BJ3505, Vtc3-6gly-3HA-G418	this study
BY4742	MATα his3Δ1 leu2Δ0 lys2Δ0 ura3Δ0	(Brachmann et al., 1998)
BY4742 *ppx1*Δ *ppn1*Δ	BY4742, ppn1::kanMX ppx1::natNT2	this study
BY4742 *vtc4*Δ *ppn1*Δ	BY4742, vtc4::kanMX ppn1::natNT2	this study
BY4742 *vtc4*Δ *ppn1*Δ *VTC4*^{R264X}	BY4742, vtc4::kanMX ppn1::natNT2 pRS303-P_{Vtc4}-Vtc4^{R264X}; X= R, A	this study
BY4727 *vtc1*Δ VTC1^{X}	BY4727, vtc1::His1 pRS304-P_{Vtc1}-Vtc1^{Y}; Y= WT, K24E, K24S, R31E, R98E	(Hothorn et al., 2009)
BY4741	MATa his3Δ1 leu2Δ0 met15Δ0 ura3Δ0	Euroscarf
BY4741 P_{GAL} 3HA-Ppx1	MATa his3Δ1 leu2Δ0 met15Δ0 ura3Δ0 P_{GAL} 3HA-Ppx1(NAT)	this study

Supplementary information

Table S2. Primers used in this study

Name	Sequence	Targeted gene
Primers for producing gene knock-outs		
Fwd YD010	CTA CAT TAT CGA ATA CGA TTA AAC ACT ACG CCA GAT TTC CAC AAT ATG CAG CTG AAG CTT CGT ACG C	VTC1
Rev YD011	AGT TTG TGC GTA ACC CAC GCT TAC GAT ATT GGA ATT ACA ATT TCA GCA TAG GCC ACT AGT GGA TCT G	VTC1
AS286	CTA TTG TTT TCA TTG AGT AGG GGT AGA GCT AGT TAG CTG CTT TTC GAT GCG TAC GCT GCA GGT CGA C	PPN1
AS287	AAA CTG TAA TTG AAG AAT GAT ATG CAT TTC TAT GTG TAT ATT AAC TTA ATC GAT GAA TTC GAG CTC G	PPN1
AS171	CAA ATA ATC AAA AAG TTC AAA ACA CCG ATT GTT AAG AAA GAT GCG TAC GCT GCA GGT CGA C	PPX1
AS172	GGG TCA TAT ATA AAC CAA ATA AAG CAT ATATAA CAT CTC CCT TCA ATC GAT GAA TTC GAG CTC G	PPX1
Ctrl fwd YD012	TAT CGC TTG TTA CGG TCG GT	
Ctrl rev AS12	GCC CAT TTA TAC CCA TAT	
PCR primers		
Fwd YD047	CGG GAT CCA TGA AAG CAT TCA CCA GTT TAC	PPCPY
Rev YD037	CGG AAT TCG TTG ACA CGA AGC TGA TAG TTT TC	PPCPY
Fwd YD033	CGG AAT TCT CGC CTT TGA GAA AGA CGG TT	PPX1
Rev YD044	CCG CTC GAG TCA CTC TTC CAG GTT TGA GTA	PPX1
Fwd YD070	CCC AAG CTT ATG GGT CAG GAA AAG CTA TAC	*Ec*PPK1
Rev YD039	CCG CTC GAG TTA TTC AGG TTG TTC GAG TG	*Ec*PPK1
Fwd YD069	CGG AAT TCA TGT CGC CTT TGA GAA AGA CGG TT	PPX1
Rev YD034	CCC AAG CTT TCA CTC TTC CAG GTT TGA GTA	PPX1
Fwd YD065	CGG AAT TCT CGC CTT TGA GAA AGA CGG TT	PPX1
Rev YD066	CCG CTC GAG CTC TTC CAG GTT TGA GTA CG	PPX1
Fwd YD067	CCG CTC GAG TCT AAA GGT GAA GAA TTA TTC	GFP
Rev YD068	CGA CGC GTT TAT TTG TAC AAT TCA TCC AT	GFP
Fwd YD196	CCA CTT GAA ACA AAT AAT CAA AAA GTT CAA AAC ACC GAT TGT TAA GAA AGA TGC GTA CGC TGC AGG TCG AC	P_{GAL} 3HA
Rev YD197	TTT TAA GTG TGC CAA AAA TTC AGG AAC CGT CTT TCT CAA AGG CGA CAT CGA TGA ATT CTC TGT CG	P_{GAL} 3HA
Fwd Ctrl T776	CCT CTA TAC TTT AAC GTC AAG GAG	P_{GAL} 3HA
Rev Ctrl YD035	TGC TGA CTC GTT ACC AAC ACA	P_{GAL} 3HA